JATIS Journal of Astronomical Telescopes, Instruments, and Systems

RESEARCH PAPER

Star and planet formation with the Single Aperture Large Telescope for Universe Studies space observatory

Kamber R. Schwarz[a,*] **Alexander Tielens**[b] **Joan Najita**[c] **Jennifer Bergner**[d] **Quentin Kral**[e] **Carrie Anderson**[f] **Gordon Chin**[f] **David Leisawitz**[g] **David Wilner**[h] **Peter Roelfsema**[i] **Floris van der Tak**[i] **Erick Young**[j] **and Chris Walker**[k]

[a]Max-Planck-Institut für Astronomie, Heidelberg, Germany
[b]University of Maryland, Astronomy Department, College Park, Maryland, United States
[c]NSF's NOIRLab, Tucson, Arizona, United States
[d]University of California, Berkeley, Berkeley, California, United States
[e]Université PSL, Sorbonne Université, Université Paris Cité, CNRS, LESIA, Observatoire de Paris, Meudon, France
[f]NASA Goddard Space Flight Center, Planetary Systems Laboratory, Greenbelt, Maryland, United States
[g]NASA Goddard Space Flight Center, Observational Cosmology Laboratory, Greenbelt, Maryland, United States
[h]Center for Astrophysics Harvard Smithsonian, Cambridge, Massachusetts, United States
[i]Netherlands Institute for Space Research (SRON), Groningen, The Netherlands
[j]Universities Space Research Association, Washington, DC, United States
[k]University of Arizona, Department of Astronomy and Steward Observatory, Tucson, Arizona, United States

ABSTRACT. The Single Aperture Large Telescope for Universe Studies (*SALTUS*) is a far-infrared space mission concept with unprecedented spatial and spectral resolution. *SALTUS* consists of a 14-m inflatable primary, providing 16× the sensitivity and 4× the angular resolution of *Herschel*, and two cryogenic detectors spanning a wavelength range of 34 to 660 μm and spectral resolving power of $300 - 10^7$. Spectroscopic observations in the far-infrared offer many unique windows into the processes of star and planet formation. These include observations of low-energy water transitions, the H_2 mass tracer HD, many CHONS constraining molecules such as NH_3 and H_2S, and emission lines from the phonon modes of molecular ices. Observing these species will allow us to build a statistical sample of protoplanetary disk masses, characterize the water snowline, identify Kuiper Belt-like debris rings around other stars, and trace the evolution of CHONS from prestellar cores, through to protoplanetary disks and debris disks. We detail several key star and planet formation science goals achievable with *SALTUS*.

Keywords: star formation; protoplanetary disks; astrochemistry; terahertz spectroscopy; far-infrared; space telescopes

Paper 24114SS received Jul. 18, 2024; revised Oct. 17, 2024; accepted Oct. 21, 2024; published Nov. 15, 2024.

1 Introduction

The Single Aperture Large Telescope for Universe Studies (*SALTUS*) is a far-infrared space mission concept proposed to NASA under the Astrophysics Probe Explorer (APEX) Announcement

*Address all correspondence to Kamber R. Schwarz, schwarz@mpia.de

of Opportunity in November 2023. *SALTUS* covers the far-infrared wavelength range ≈30 to 700 μm, most of which is not covered by any current observatory. The design of *SALTUS* consists of a 14-m off-axis inflatable primary aperture and two cryogenic instruments: SAFARI-Lite and the High-Resolution Receiver (HiRX). The large aperture size allows for unprecedented sensitivity and a spatial resolution of $\sim 1''$ at 50 μm. The full technical details of the *SALTUS* observatory can be found in Arenberg et al., "Design, Implementation and Performance of the Primary Reflector for SALTUS"; Kim et al., "SALTUS Observatory Optical Design and Performance"; and Donovan et al., "SALTUS Probe Class Space Mission: Observatory Architecture & Mission Design," *J. Astron. Telesc. Instrum. Syst.* (this issue). SAFARI-Lite is a direct-detection grating spectrometer providing simultaneous 35 to 230 μm spectroscopy with a resolving power of $R = 300$. The full technical details can be found in Roelfsema et al., "The SAFARI-Lite Imaging Spectrometer for the *SALTUS* Space Observatory," *J. Astron. Telesc. Instrum. Syst.* (this issue). HiRX is a multi-pixel, multi-band heterodyne receiver system spanning wavelength ranges 522 to 659 μm, 136 to 273 μm, 111.9 to 112.4 μm, 63.1 to 63.4 μm, and 56.1 to 56.4 μm with a resolving power of $R = 1 \times 10^5 - 1 \times 10^7$. The full technical details can be found in Walker et al., "The High Resolution Receiver (HiRX) for the Single Aperture Large Telescope for Universe Studies (SALTUS)," *J. Astron. Telesc. Instrum. Syst.* (this issue).

SALTUS bridges the gap in wavelength coverage between JWST-MIRI (4.9 − 27.9 μm) and ALMA (320 to 8500 μm). Crucially, *SALTUS* covers the ground state H_2O and HD lines not currently covered by any facility. While there is an overlap between HiRX Band 1 and ALMA Band 8, the Earth's low atmospheric transmittance at these wavelengths, particularly near the HDO lines targeted by *SALTUS* makes observations from the ground difficult. The difficulties of atmospheric transmittance can be mitigated through the use of balloon experiments such as BLAST and GUSTO.[1,2] However, such experiments have several notable limitations. They are currently limited to flights in Antarctica and thus can only observe the southern sky. In addition, the limited flight time and limited apertures preclude long integrations on faint sources. As such, balloon experiments are best suited to surveys of large-scale structures. Targeted observations of faint objects require a pointed observatory.

This paper provides an overview of the promise of *SALTUS* for understanding star and planet formation, including molecular clouds, protostellar cores, protoplanetary disks, and debris disks. Accompanying papers in this issue describe the plans for guaranteed-time (GTO) and guest observing (Chin et al., "Single Aperture Large Telescope for Universe Studies (SALTUS): Probe Mission and Science Overview," *J. Astron. Telesc. Instrum. Syst.*), SALTUS' contributions to High-Redshift Science (Spilker et al., "Distant Galaxy Observations," *J. Astron. Telesc. Instrum. Syst.*), Milky Way and nearby galaxies science (Levy et al., "Nearby Galaxy Observations" *J. Astron. Telesc. Instrum. Syst.*), and solar system observations (Anderson et al., "Solar System Science" *J. Astron. Telesc. Instrum. Syst.*). In addition, some of *SALTUS*'s key science cases build on the *OASIS* MIDEX-class mission concept, which used a similar large inflatable aperture for terahertz frequency observations.[3]

1.1 Programmatic Motivation

The *SALTUS* star and planet formation science programs presented here address multiple high-priority science questions as identified by Astro2020,[4] detailed below.

- Question E-Q1c: *How Common Is Planetary Migration, How Does It Affect the Rest of the Planetary System, and What Are the Observable Signatures?* This section of the Astro2020 report notes that C/O ratios in exoplanet atmospheres can be used to determine a planet's formation location relative to the snowlines in its parent disk, but only if the disk composition, particularly the location of the water snowline, is well understood. *SALTUS* will provide the disk water measurements, including measurements of the water snowline location, needed to connect atmosphere compositions to the water distribution of planet-forming disks and thereby connect JWST observations of exoplanet atmospheres to a formation time and location (Sec. 2.2).
- Question E-Q1d: *How Does the Distribution of Dust and Small Bodies in Mature Systems Connect to the Current and Past Dynamical States Within Planetary Systems? SALTUS* SAFARI-Lite will determine the occurrence of exo-Kuiper belts around the nearest 30 G

and K stars known to host debris disks, characterizing the commonality of dust in mature planet systems (Sec. 2.6.1).

- Question E-Q3a: *How Are Potentially Habitable Environments Formed? SALTUS* will answer this question by observing secondary gas in debris disks in the form of [CII] at 157 μm and [OI] at 63 and 145 μm in debris disks, tracing the C/O ratio of material available for accretion onto terrestrial planets (Sec. 2.6.2).
- Question E-Q3b: *What Processes Influence the Habitability of Environments?* and Question F-Q4b: *What Is the Range of Physical Environments Available for Planet Formation? SALTUS* will determine the mass and temperature structure, as well as the abundance of CHONS-bearing species, in roughly 1000 protoplanetary disks across evolutionary stages (Secs. 2.1.1, 2.2, and 2.4.1).

2 Star and Planet Formation Science with SALTUS

2.1 Protoplanetary Disk Mass

One of the most fundamental properties of planet formation is the mass of a planet-forming disk, which determines the total amount of material available to forming planets and the mechanisms through which planets can form, e.g., through gravitational instability versus via core accretion.[5] The main contributor to the disk mass is H_2, which does not emit for the majority of disk regions because the molecule has no permanent dipole moment, with large energy spacings not well matched to the local temperatures. The ground-state transition is the quadrupole $J = 2$-0 with an energy spacing of 510 K. Thus, exciting an H_2 molecule to the $J = 2$ state requires high gas temperatures and H_2 emission originates only from the illuminated surface layers of the disk within a fraction of an au of the central star. Because most of the gas is at larger radii and is much colder, alternate tracers must be used to determine the total gas mass.

The most commonly used gas mass tracers in protoplanetary disks are continuum emission from dust and emission from rotational transitions of CO. Each method relies on different problematic assumptions. Uncertainties in the dust grain optical properties and the grain size distribution lead to significant uncertainty in the derived dust mass from observed emission. Then, to convert from dust mass to gas mass, a gas-to-dust mass ratio must be assumed. This value is typically assumed to be 100, as has been measured in the interstellar medium (ISM).[6] However, several factors can change this ratio in disks, including loss of gas due to disk winds and accretion onto the central star, which will decrease the gas-to-dust ratio, and growth of dust grains beyond cm sizes, at which point the dust emission is no longer observable. In addition, assuming a constant gas-to-dust ratio across the disk is not appropriate because high spatial resolution observations at millimeter wavelengths demonstrate that the outer radius of the dust disk is often much smaller than the outer radius of the gas disk.[7,8]

The CO abundance relative to H_2 in the ISM is well constrained to be 5×10^{-5} to 2×10^{-4}.[9] However, when converting from CO abundance to H_2 in a protoplanetary disk, additional corrections must be made to account for the reduced abundance of CO relative to H_2 in the surface layer, where CO is photo-dissociated, and near the cold midplane, where CO is frozen out onto dust grains.[10] Additional chemical reactions in the gas and on dust grains can also destroy CO.[11] The resulting reduction in CO gas abundance, whatever the cause, varies not only across sources but also as a function of radius within a single disk.[12] Thus, there are large uncertainties when converting CO flux to total gas mass.[13] These uncertainties can be particularly mitigated by additional observation of N_2H^+, which, being destroyed by reacting with CO, is only present in the gas when CO is not.[14,15] However, this technique requires knowing the ionization state of the protoplanetary disk, a property that remains poorly constrained for most systems.[16–18] A detailed discussion of all the common disk mass estimation techniques can be found in Ref. 13.

Given the myriad assumptions that go into each technique, it is not surprising that the two methods of determining disk mass rarely agree. Alternative mass probes, preferably requiring fewer assumptions, are needed to determine the true disk gas mass. One possibility is to use the disk rotation curve to constrain the enclosed mass (e.g., Ref. 19). However, because disks must always be less massive than the central star to remain gravitationally stable, the contribution of the disk to the rotation curve is small. This technique is only feasible for a small number of the most massive disks.[20]

2.1.1 *Tracing mass with HD*

SALTUS will use HD to measure the gas mass in hundreds of disks, establishing the variation in this fundamental parameter across systems. Observations of the H_2 isotopologue HD are unique to the far-IR, with the ground state 1-0 rotation transition at 112.07 μm (2.675 THz; SAFARI-Lite LW Band, HiRX-Band 3) and the 2-1 transition at 56.24 μm (5.331 THz; SAFARI-Lite MW Band, HiRX-Band 4b). HD is the main reservoir of deuterium, and its abundance relative to H_2 will be close to the elemental D/H abundance; thus, HD can be used to trace disk mass while avoiding many of the limitations of other mass tracers. For example, HD emission is not subject to chemical processing that can change the abundances of other tracers relative to H_2.[21] The HD 1-0 line is expected to remain optically thin for disks less massive than $1 \times 10^{-3}\,M_\odot$ while HD 2-1 remains optically thin up to $2.3 \times 10^{-2}\,M_\odot$.[22] Observations of only the HD 1-0 are capable of constraining the disk mass to within a factor of 2-10 depending on disk mass, whereas the additional observation of the HD 2-1 line decreases this uncertainty to no more than a factor of 3.[22,23] *SALTUS* HiRX is designed to observe both lines simultaneously.

There is currently no observatory capable of detecting HD. Near the end of its lifetime, Herschel targeted HD in seven massive disk systems, resulting in three detections,[7,8] with HD-derived disk gas masses of $30 - 210\,M_J$ (e.g., Ref. 24). Crucially, these mass measurements revealed that both CO and H_2O gas are depleted in these disks relative to the ISM.[9,25] *SALTUS* SAFARI-Lite will measure the total gas mass in hundreds of protoplanetary systems over its 5-year baseline mission, down to masses as low as $0.1\,M_J$ (Fig. 1). When combined with observations of cold water vapor, this determines the amount of water removed from the outer disk and transformed into water ice in the planet-forming midplane (see also Ref. 26).

Converting the HD detections into an accurate total gas mass requires knowledge of the disk temperature structure, as HD does not emit appreciably below 20 K. The *SALTUS* design allows for full spectral coverage with SAFARI-Lite or simultaneous observations in the four HiRX bands. While integrating on the HD 1-0 and 2-1 lines in HiRX-3,4b, *SALTUS* is able to observe multiple optically thick H_2O and CO lines in HiRX-1,2 spanning 55 to 1729 K in excitation energy, compared with 128.49 K for the HD $J = 1$ excited state. In addition, *SALTUS* will observe [O I] and [C II], which trace the hotter disk surface and are important cooling lines.[27,28] These lines provide direct measurements of the gas temperature throughout the disk.

The high spectral resolution of HiRX can then be used to map emissions to different physical locations in the disk using a technique known as Doppler tomography or tomographic mapping. Because disk rotation follows a Keplerian velocity profile, the radius at which gas emission originates can be determined from the line profile. Thus, high spectral resolution observations of molecular lines in disks can be used to determine the radial location of the emission without

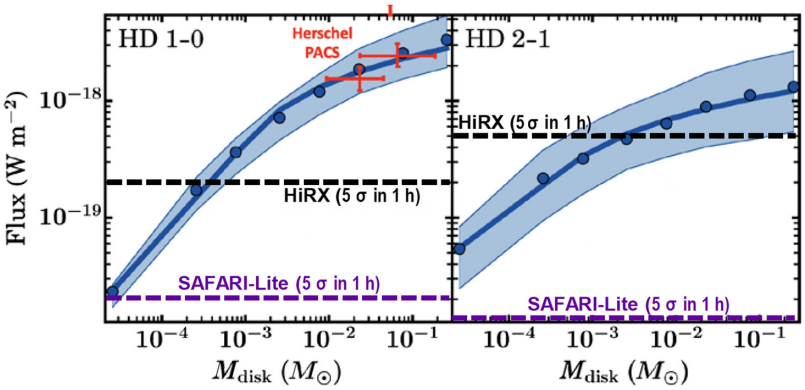

Fig. 1 Model predictions of disk gas ($D = 140$ pc), as a function of HD line flux. The width of the blue band represents the range of model results for different disk structures. The three red points represent the only known HD detections from Herschel-PACS. *SALTUS* SAFARI-Lite will make observations for the full range of fluxes plotted, with 5σ, 1-h sensitivities between 0.5 and 2×10^{-20} W m^{-2} across the four bands. SALTUS HiRX will be sensitive enough to provide high spectral resolution observations, with 5σ, 1-h sensitivities $>5 \times 10^{-19}$ W m^{-2} in $J = 2$-1 and $>2 \times 10^{-19}$ W m^{-2} in $J = 1$-0. Figure modified from Ref. 22.

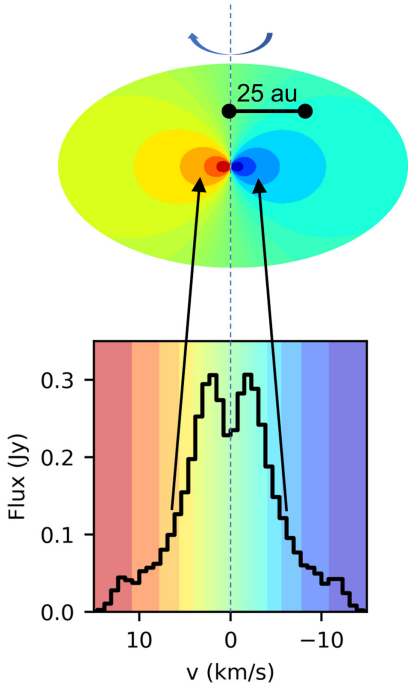

Fig. 2 A simulated disk-integrated spectrum of HD 1-0 for a 10^{-3} $M_\odot$ disk at a distance of 140 pc, inclined by 45 deg. The spectral resolution is $\Delta v = 0.9$ km s^{-1}. Disk emission is Doppler shifted due to Keplerian rotation. Emission with a high-velocity offset from the line center originates from small radii, whereas emission close to the systemic velocity originates from large radii. The HiRX high spectral resolution enables differentiation between emissions from different radii in protoplanetary disks.

having to spatially resolve the disk. As shown in Fig. 2, the velocity offset for emission originating in the inner disk is of order several km s^{-1} assuming a disk inclination of 45 deg, whereas in the outer disk, the velocity offset is much smaller. The velocity resolution (Δv) of SALTUS HiRX is <1 km s^{-1}, sufficient to distinguish emission originating in the inner versus outer disk.

Taking the expected HD fluxes and line-to-continuum values into account from Fig. 1,[22] SAFARI-Lite measures the $J = 1$-0 and 2-1 lines at the 5σ level in 1 h for the limits provided in Fig. 1, enabling reliable disk gas mass estimates. For a survey of disk mass across systems, which requires only the total HD flux, spectrally unresolved observations with SAFARI-Lite are able to quickly build a catalog of HD detections. The expected continuum flux from a 3×10^{-5} $M_\odot$ disk at 140 pc, where many young stars are found, is 0.02 Jy.[22] SNR of 300 requires a sensitivity of 66 μJy at 112 μm, the wavelength of the HD 1-0 transition. Based on the modeled grating sensitivity of SAFARI-Lite (Roelfsema et al., this issue), this can be achieved in less than an hour on the source. SAFARI-Lite's greater sensitivity at 54 μm, the wavelength of the HD 2-1 transition, achieves SNR 300 in even less time. Using the sample collected by Ref. 29, roughly 300 disks will be detected in HD by *SALTUS* SAFARI-Lite in less than 1 h, including ~200 disks where HD 2-1 is optically thin and an additional ~50 where both transitions are optically thin.

For a subset of the brightest disks, HiRX spectrally resolves the strong HD lines at a 1 km s^{-1} velocity resolution to measure the line profile in detail and use Doppler tomography to constrain the disk structures. As shown in Fig. 2, the velocity offset for emission originating in the inner disk is of order several km s^{-1} assuming a disk inclination of 45 deg, whereas in the outer disk, the velocity offset is much smaller. The velocity resolution of SALTUS HiRX is <1 km s^{-1}, sufficient to distinguish emission originating in the inner versus outer disk. As an example, TW Hya, with a disk mass of 0.025 $M_\odot$ and a nearly face-on inclination has a peak HD 1-0 flux of 0.49 Jy when placed at a distance of 140 pc.[24] *SALTUS* HiRX Band 3 yields a 5σ detection at $\Delta v = 1$ km s^{-1} in 20 h. More inclined disks will have more flux in the line wings, as the observed velocity offset is directly proportional to $\sin(i)$. Based on dust mass

measurements and assuming a gas-to-dust ratio of 100, we expect to achieve equivalent or greater signal-to-noise on at least 15 disks within 140 pc.[29] We can expect to observe five targets per year in the tomographic mode if we allocate 100 h per year to these observations. These deep HiRX observations of sources spanning several arcseconds in the sky will also provide constraints on the spatial extent of the line emission for these disks, important for validating the models used for interpretation of surveys. In total, *SALTUS* will obtain the disk gas masses in hundreds of protoplanetary systems during its nominal 5-year mission without the need for ancillary data.

2.2 Spatial Distribution of Water in Protoplanetary Disks

SALTUS will be the first mission with the sensitivity to measure the distribution and physical properties of water in a large sample of protoplanetary disks. These measurements are key for understanding planet formation and how terrestrial planets acquire water. The *SALTUS* instruments are designed to probe both the gas and the solid H_2O reservoirs and relate them to the characteristics of the central protostar (luminosity, spectral type) and of the planet-forming disk (evolutionary state, mass, structure, temperature). The large frequency range of HiRX and SAFARI-Lite provides access to many H_2O lines with a wide range of excitation energies, tracing the cold-to-warm water vapor in disks, addressing Decadal Questions E-Q1c, E-Q3b, and F-Q4b.

The first part of this program focuses on water vapor. *Herschel* revealed tantalizing but tentative and limited evidence of water removal from the surface layers of outer disks.[30,31] *SALTUS*'s large improvement in sensitivity relative to *Herschel* makes observations of water in disks routine and enables a complete survey of water in all protoplanetary disks within 200 pc. This large number of observations will allow *SALTUS* users to conclusively identify trends between the distribution of water in disks and other properties, e.g., dust disk size and the presence of substructure.[32]

Question E-Q1c from the 2020 decedal asks: "How common is planetary migration, how does it affect the rest of the planetary system, and what are the observable signatures?" The composition of a planet's atmosphere is related to the composition of the disk where and when it accreted its material and can be used to determine if a planet could have formed at its current location or must have migrated. The chemical composition of the disk at a given location evolves over time due to both chemical and dynamical processes.[33] Current observational studies aim to use atmospheric C/O to differentiate between early and late migration of Hot Jupiters.[33] Models of how migration changes C/O in a planet's atmosphere make simplifying assumptions for C/O in the disk.[34] The main volatile oxygen reservoir in disks, water, is virtually unconstrained by observations. *JWST* is already significantly improving our understanding of water in the mid-IR.[35–38] However, as noted by Decadal Question E-Q1c, additional longer wavelength observations of cooler regions of the disk are needed to understand disk composition. HiRX will map the radial distribution of cold water vapor in hundreds of protoplanetary disks. These disks will span a wide range of stellar mass and mass accretion rate, disk dust mass, and disk radial extent, and span multiple star-forming regions, covering a variety of evolutionary stages[29] HiRX will observe the cold water vapor (not probed by *JWST*) by targeting the ground state ortho and para transitions (Fig. 3), allowing users to collect statistics on the cold water abundance in disks across evolutionary stages. Figure 3 shows the model far-IR spectrum of a protoplanetary disk at a distance of 160 pc. The lines have been scaled to match the H_2O lines detected in TW Hya by Herschel, as well as the HD line, if that disk was at a distance of 160 pc.[7,30] Comparison to models shows the cold H_2O in TW Hya to be depleted by about a factor of 100.[9] SAFARI-Lite can detect a 0.5×10^{-20} to 2×10^{-20} W m^{-2} line at 5σ with 1 h of integration time, depending on the band. Thus, surveys of water in star-forming regions at 160 pc, such as Taurus and Lupus, will be able to detect cold H_2O vapor in many systems. *SALTUS* will provide the disk water measurements needed to connect *JWST* observations of exoplanet atmospheres to a formation time and location.

SALTUS will tomographically map the water vapor distribution toward a wide variety of disks, answering the question "Where is the water?" Mapping the location of water in protoplanetary disks is crucial for understanding the transport of water during planet formation.[4] Current planet formation models predict that most planets form beyond the snowline (gas/ice giants and possibly smaller planets) and then experience radial migration and dynamical scattering.[40] Confirming this prediction requires observational constraints on the water snowline

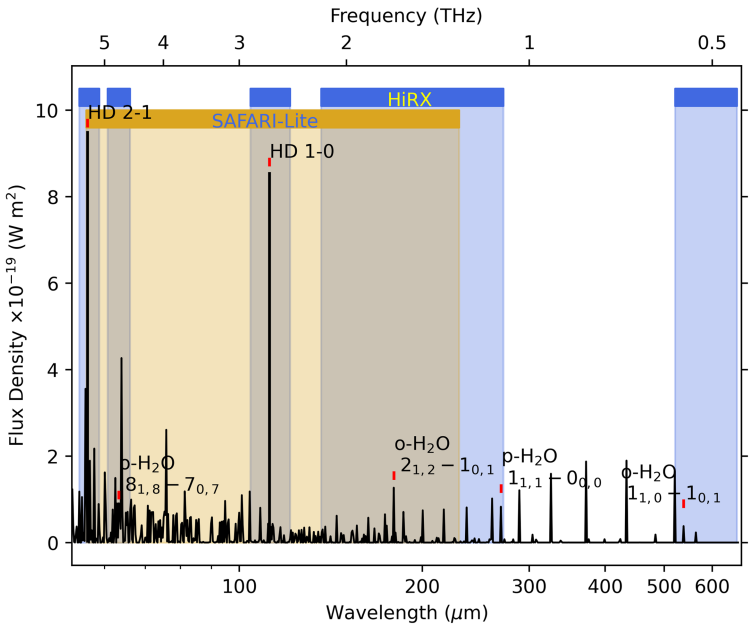

Fig. 3 The HiRX and SAFARI-Lite instruments will measure the gaseous emission spectrum of planet-forming disks, thereby determining unambiguously the disk gas mass, the water content, and the HDO/H_2O abundance ratios; all critical aspects of disk/planet formation models. Model emission lines are for TW Hya, a water-depleted disk, scaled to a distance of 160 pc, adapted from Ref. 39. The far-IR provides access to low energy transitions that probe the cold, outer parts of the disk of the planet-forming reservoir.

location as functions of, e.g., disk mass, stellar mass, and evolutionary state, to compare with the orbital radii of exoplanets in mature systems.

The ice snowline, the H_2O desorption front located at ~150 to 170 K in the disk, controls the radial distribution of the C/O ratio in the gas and solid phase,[34] implying that the spectral characteristics of planets are linked to their formation location. Water on terrestrial planets that formed within the snow line (including Earth) is thought to have been at least partially delivered by comet and asteroid impacts originating from cold disk reservoirs beyond the snow line.[41] As the mass of solids is expected to be the largest near the snow line, the formation of giant planets, such as Jupiter, is generally linked to the location of the snow line in the solar nebula. Giant planet formation may be aided by the increased "stickiness" of H_2O ice grains relative to minerals, which greatly enhances the coagulation of small dust grains[42]—the first step in planet formation—in the colder regions of these disks.

SALTUS will probe the midplane water snowline location by observing multiple high upper-state energy ($E_u \sim 1000$ K) water lines, which emit mostly from inside the midplane water snowline.[43] Using tomographic mapping, *SALTUS* will determine if water is returning to the gas with the inward drift of icy dust grains, enriching the water content of the terrestrial planet-forming region. By contrast, *JWST* primarily probes higher energy emission lines, with upper-state energies of several hundred to over a thousand Kelvin.[36,38] In addition, the dust continuum in the inner disk at mid-IR wavelengths is optically thick, such that the H_2O emission observable by *JWST* originates near the disk surface.[44] In the far-IR, the optically thick dust layer is deeper in the disk, and the lower upper state energy of the water lines probe deeper in the disk, (z/r of $0.1 - 0.2$ au for a typical T-Tauri disk[43]). However, the midplane remains optically thick. Due to dust optical depth, this problem cannot be overcome by observing rarer H_2O isotopologues. Direct measurements of the water emitting radius via tomographic mapping provide an upper limit on the midplane snowline location, which can be further refined using models of the disk temperature structure.[25] In addition, some models predict efficient vertical mixing of gas at small radii.[45,46] This results in a nearly vertical water snow surface, meaning the snowline directly probed by *SALTUS* observations is equivalent to the midplane snowline location. *SALTUS* will make the first measurements of the disk midplane water snowline location in non-outbursting

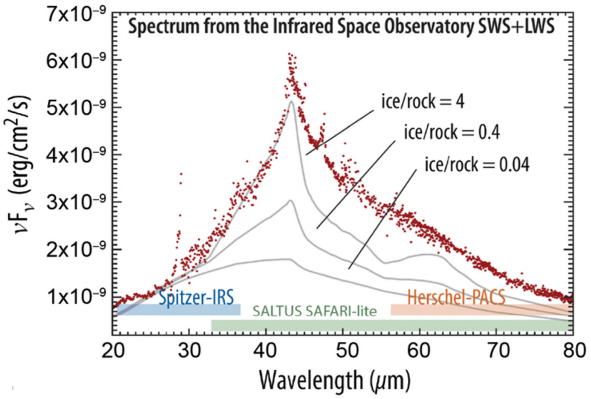

Fig. 4 The far-IR spectrum of the Herbig star, HD 142527, measured by ISO/SWS+LWS and Herschel/PACS (red points), reveals the presence of the lattice modes of crystalline H_2O ice at 43 and 62 μm.[49] This is compared with emission models at different ice/rock ratios (gray lines). The tell-tale signature of crystalline water ice is recognizable to ice/rock ratios as small as 0.1. For comparison, the estimated ice/rock ratio in the solar nebula during planet formation is 1-2.

disks, an important landmark in the core accretion picture. *SALTUS* enables us to assess the role of the water snowline in determining the architecture of planetary systems (i.e., Refs. 47 and 48), and the extent to which processes (e.g., migration, dynamical scattering) alter exoplanetary orbital radii; this addresses Decadal Question E-Q1c.

The second part of the program will target water ice directly. Water ice is the most abundant non-refractory solid-state component of planet-forming disks, locking up a major fraction of the elemental oxygen. The water ice distribution in protoplanetary disks is of fundamental importance for our understanding of planet formation and their characteristics. As a result of its simultaneous spectral coverage of the full 34 to 230 μm range and its high sensitivity, SAFARI-Lite is uniquely suited to study emission in the diagnostic lattice modes of ices in protoplanetary disks (Fig. 4), providing temperature, mass, and structure of the emitting ices. Previous far-IR space missions (*Spitzer*, *Herschel*, *ISO*) lacked the wavelength coverage or sensitivity for a systematic study of far-IR ices, especially in planet-forming disks. While the NIRSpec and MIRI instruments on *JWST* cover the near- and mid-IR region, home to ice fundamental modes, these shorter wavelengths require a very favorable viewing angle—almost edge-on—and cannot perform a systematic study of the role of ices in planet-forming disks. Further, because these features are seen in absorption, they provide only a lower limit on the absorbing column, as a photon's path as it is scattered through the disk is uncertain.[37,50] The far-IR features have the advantage of being seen in emission and are therefore not subject to the same constraints due to viewing angle and scattering.

The large wavelength coverage and moderate spectral resolution of SAFARI-Lite are well matched to the expected profile variations in the lattice modes of H_2O ice, measuring the temperature history of the ice grains. This is linked to a physical location through models of disk temperature structure, constrained by the H_2O gas observations. The gas and solid reservoirs interact through sublimation and condensation as icy grains drift inwards from the cold outer disk to the warm inner disk and through turbulent cycling between the colder mid-plane and the warmer disk photosphere. *SALTUS* will quantify the mass of the gaseous H_2O and ice reservoirs in a large sample of protostellar and protoplanetary sources, assess the interrelationship of these reservoirs, and connect them to the physical characteristics of the stars and their disks and thereby address the importance of the physical processes that link them.

2.3 Water in Prestellar Cores

Prestellar cores are the gravitationally bound phase of star formation immediately prior to the protostar formation,[51–53] with cold ($T < 10$ K), dense ($n > 10^5$ cm^{-3}) central regions that are well shielded from the surrounding interstellar radiation field. During this phase, the initial chemical conditions are set for the disk and subsequent planet formation. The direct chemical

inheritance from the prestellar phase to the protostellar disk has been established, e.g., reflected in the D/H ratio from ALMA observations of deuterated water.[54]

Although most of the water in prestellar cores resides in the solid state on the dust grain icy surfaces,[55] photodesorption by UV photons can liberate water molecules into the gas phase at abundances that are typically $<10^{-9}$ with respect to H_2.[56] Two main sources of UV photons exist: the surrounding interstellar radiation field is the dominant heating component of dust grains[57] and a low-intensity UV radiation field from H_2 excitation due to collisions with electrons that come from cosmic ray ionizations of H_2 and He.[58]

The $1_{10} - 1_{01}$ ground state rotational transition of ortho-H_2O at 538.2 μm (557 GHz; HiRX 1) can be observed in absorption against the continuum of the prestellar core.[56] The line can also be seen in emission if the central density of the prestellar cores is $>10^7$ cm^{-3}, although only a few prestellar cores are known that have this extreme central density.[59] The gas phase water in the outer part of the core at low A_V has a photodesorption rate that depends on the strength of the interstellar radiation field (G_0), and a constraint on G_0 is needed to determine the dust temperature and the gas temperature profiles in the outer part of prestellar cores.[60] Accurate temperature profiles are crucial for radiative transfer modeling of molecular emission and absorption observed toward prestellar cores, and *SALTUS* water vapor observations of prestellar cores will play an important role in constraining the temperature profile in the outer part of the cores.

2.4 Astrochemistry: CHONS From Cores to Disks

Hot cores are hot molecular line emission regions within massive star-forming regions, typically characterized by high temperatures (100 s of K) and densities ($\sim 10^7$ cm^{-2}).[61] Originally identified from the detection of hot NH_3 toward Orion-KL,[62] hot cores were subsequently found to host an incredibly rich gas-phase organic chemistry.[63] Ice mantles are the main sites of astrochemical complex organic molecule formation, and ice sublimation is the source of the chemical complexity detected in hot cores.[64,65] Observing molecular line emission from hot cores provides powerful constraints on their physical and chemical conditions.[66]

SALTUS's high sensitivity at far-IR wavelengths will open a new window into studying complex organic molecules in hot cores. Figure 5 illustrates how a massive star-forming region can appear line-poor with *Herschel* but harbor hundreds of spectral lines when observed with a higher sensitivity and resolution observatory (ALMA Band 10). The ALMA observations in Fig. 5 have a spectral resolution of 0.5 km s^{-1}. Similarly, *SALTUS*'s HiRX instrument will have a sub-km s^{-1} resolution, e.g., 0.66 km/s in HiRX Band 2, allowing us to identify individual lines, even in crowded spectral regions. We similarly expect higher line densities of organics with *SALTUS* compared with Herschel. While the sensitivity increase with *SALTUS* will be more modest than with ALMA, we note that ALMA Band 9 and 10 observations require exceptional weather conditions and do not extend to wavelengths shortward of 315 μm, whereas *SALTUS* will provide access to wavelengths as short as 34 μm.

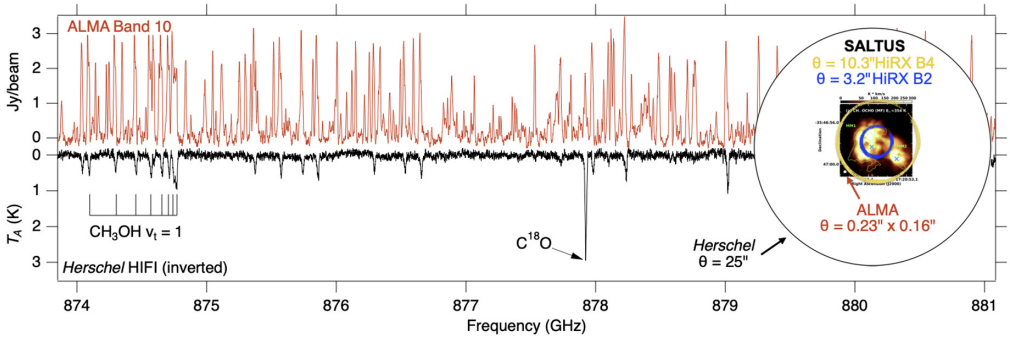

Fig. 5 Comparison of observations of the high-mass star formation region NGC 6334I taken with ALMA (red) and Herschel (black and inverted). The inset shows the beam size for Herschel, ALMA, and *SALTUS* overlayed on a methyl formate intensity map of the region. The effects of beam dilution will be much less severe with SALTUS than with Herschel. Figure adapted from Refs. 67 and 68.

While many complex organics can be detected at longer wavelengths, there are several advantages to obtaining far-IR observations. First, the lines covered by *SALTUS* typically probe higher upper-state energies than millimeter-wavelength lines, which can better constrain excitation conditions. This is especially important for high-mass hot cores, in which organics often have excitation temperatures of a few 100 K.[69,70] Constraints on organic molecule excitation temperatures are required to interpret the physical conditions of the emitting regions, as well as the chemical relationships between different classes of molecules (see also Ref. 67).

The early Class 0 and I stages of low-mass protostellar evolution, characterized by an infalling envelope of gas and dust, are often accompanied by an outflow, which promotes accretion onto the protostar by carrying away angular momentum. Encounters between the outflow and the ambient envelope material produce shocks, which can alter the local chemistry through heating and grain sputtering. In some "chemically rich" outflows, the gas-phase abundances of molecules associated with the ice phase (H_2CO, CH_3OH, and CH_3OCHO) are enhanced due to shock-induced ice sputtering.[71–74] Thus, these chemically rich outflows offer a valuable window to probe the organic composition of interstellar ices. Moreover, studies of outflow shock physics and chemistry inform our understanding of the same processes that take place on smaller, disk-forming scales within the protostellar core.

The archetypical chemically rich outflow shock, L1157-B1, was observed as part of the *Herschel* CHESS survey.[75] The 471 to 540 μm spectrum contained emission lines from high-excitation transitions of grain chemistry tracers such as NH_3, H_2CO, and CH_3OH.[76] An excitation analysis revealed that these lines emit with temperatures $\geq$200 K, intermediate between the cold emission observed by longer-wavelength transitions and the very hot gas traced by H_2 emission. Thus, observations of higher-excitation organics towards outflow shocks can help link these different emission regimes and disentangle how the shock chemistry and physics progress (Fig. 6). These insights can in turn be used to refine models of shock astrochemistry, which are needed to connect observed gas-phase abundances to the underlying grain compositions.[78]

Finally, chemically rich outflow shocks are the only low-mass star-forming regions where phosphorus carriers have been detected.[79,80] In shock chemistry models, PH_3 and smaller P-bearing hydrides are predicted to be at least as abundant as the P carriers PN and PO.[81] PH_3 has only one strong transition observable longward of 600 μm and remains undetected in star-forming regions. *SALTUS*'s broad spectral coverage measurements allow for a more complete inventory of the volatile phosphorus carriers in star-forming regions.

2.4.1 *Astrochemistry: CHONS in disks*

While molecules observable at millimeter wavelengths have been extensively studied in disks, there are almost no constraints on the inventories of light hydrides in disks, many of which are observable only at submillimeter/far-IR wavelengths. Perhaps the most exciting observations of light hydrides enabled by *SALTUS* are observations of NH_3. Indeed, the N budget in disks is poorly constrained given that the dominant N carrier, N_2, cannot be directly observed in the gas. Ice spectroscopy towards low-mass protostars, the evolutionary progenitors of disks, has revealed that NH_3 is an important N carrier in the ice, with relative abundances of ~5% with respect to H_2O compared with <1% in nitriles, or XCN.[82] While nitriles are commonly detected towards disks (e.g., Refs. 83–87), NH_3 has only been detected toward two disks. The 524.1 μm transition of o-NH_3 was first detected by *Herschel* toward the nearby TW Hya disk,[88] and NH_3 was also detected towards the embedded (Class I) disk GV Tau N at mid-IR wavelengths tracing hot emission from the inner few au.[89] HiRX Bands 1 and 2 will cover multiple strong transitions tracing cool NH_3 (upper state energies 27 to 170 K). The ngVLA will also be able to observe low energy NH_3 (upper state energies 23 to 64 K), probing coldv NH_3.[90] If, similar to cold water, the abundance of cold NH_3 is low in disks, the ngVLA will detect NH_3 in few disks. *SALTUS* is sensitive to strong NH_3 transitions with upper state energies of 150 K and will probe the warm inner disk where NH_3 ice has been released into the gas.

SALTUS observations of multiple NH_3 lines will allow for the first NH_3 excitation analysis in the outer disk. In addition, *SALTUS*'s high spectral resolution will enable a kinematic analysis of the NH_3 line profiles in sources with high SNR, providing constraints on the spatial origin of

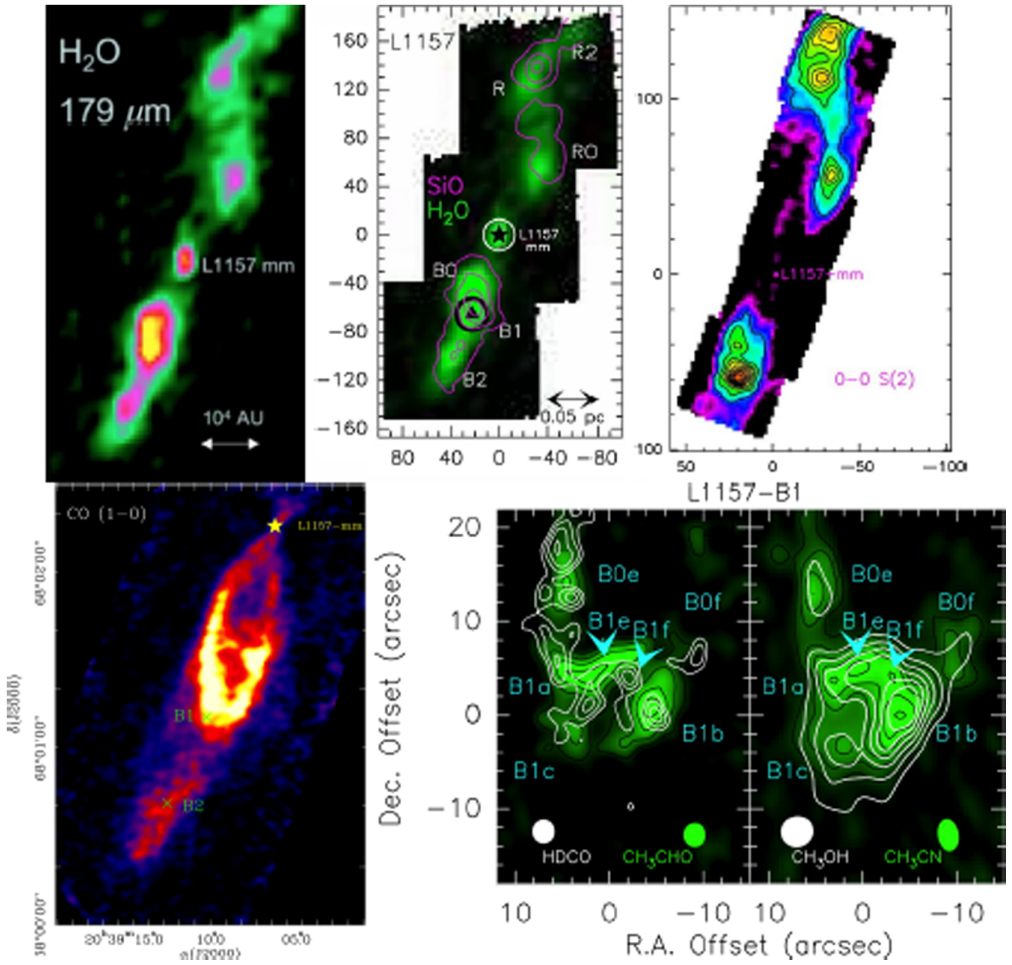

Fig. 6 Observations of an outflow from a low-mass protostar. Top left: H_2O distribution as measured by *Herschel* in the $2_{12} - 1_{01}$ transition. Top center: SiO contours overlayed on the H_2O map. Top right: Pure rotational H_2 emission from the $S(2)$ transition. Bottom left: Blue-shifted outflow lobe in CO $J = 2$-1. Bottom right: Blow up of the B1 shock at 1″ spatial resolution in acetaldehyde with HDCO contours (left) and methyl cyanide with methanol contours (right). At high spatial resolution, the outflow resolved into many small dense clumps with very distinct and highly variable chemical composition. Figure from Ref. 77.

the emission and the location of the NH_3 snowline. Auxiliary constraints on the disk structures, provided by *SALTUS* observations of CO isotopologues, HD, and H_2O, will permit robust NH_3 abundance retrievals. The NH_3/H_2O abundance ratio is of particular interest, as it can be directly compared with the ratio measured in comets to provide insights into how N is inherited by solar system bodies.

Another promising avenue for disk science with *SALTUS* is S-bearing hydrides. Sulfur is commonly very depleted from the gas in dense star-forming regions, though several S carriers (CS, SO, H_2S, and H_2CS) have been detected in disks.[91–93] H_2S was only recently detected in Class II disks: first toward GG Tau A,[94] followed by UY Aur and AB Aur.[95,96] Toward other well-known disks, deep searches for H_2S have only produced upper limits.[91] To date, only the $1_{10} - 1_{01}$ line at 168.73 GHz has been targeted, which is readily observable by ground-based telescopes but also intrinsically weak compared with the higher-frequency lines covered by SALTUS. The H_2S lines at 160.7 and 233.9 μm appear particularly promising for detection in disks with *SALTUS*, particularly if the emission originates in a somewhat warm environment.

In addition to the H_2O ice phonon modes discussed above, SAFARI-Lite's broadband coverage spanning 30 to 230 μm will cover unique spectral signatures from a large number of volatile ice species, most notably N_2, O_2, CO_2, CO, CH_3OH, CH_4, H_2S, NH_3, and HCN. The uniqueness of the lattice modes enables us to clearly distinguish between the amorphous and crystalline ice

phases, opening up a window to phase transition temperatures, which ultimately informs the thermal evolution of the ice. Ice lattice modes are also the best viable way to determine the presence of homo-nuclear molecules such as O_2 and N_2, whose fundamental modes are IR inactive. The possibility to quantify the abundance of N_2 ice in protoplanetary disks is particularly interesting as N_2 is likely a major carrier of nitrogen.[97,98]

2.5 D/H Ratios as a Probe of Interstellar Heritage

Water is a key ingredient in the emergence of life and is, therefore, a key aspect in the assessment of the habitability of (exo)planets. Yet, the origin and delivery of water to habitable planets and notably Earth remains unclear. Terrestrial water could have been delivered by water-rich asteroids driven by the migration of Jupiter in the solar nebula and/or by the late heavy bombardment during a solar system-wide rearrangement.[41,99] Outgassing from the deep mantel likely also contributed to Earth's surface water.[100] The enhanced D/H ratio in standard mean ocean water (SMOW) of 1.5×10^{-4}[101] relative to the interstellar elemental D/H ratio (1.5×10^{-5}; Ref. 102) provides support for this view as deuterium fractionation is a chemical signature indicating that a fraction of water formed under cold conditions, likely at the surface of interstellar grains (Fig. 7).[126]

This anomaly would reflect the effects of chemistry at low temperatures in cold prestellar cores where the small zero-point energy difference between D- and H-bearing species can create large deuterium fractionations.[126,127] However, the observed D/H ratio in deeply embedded protostars (hot corinos)—tracing the inherited water content—is higher than the D/H ratio in Earth's water (VSMOW) by factors of 2 to 6 (purple symbols in Fig. 7). Hence, chemical processing must have occurred in warm gas, reducing the deuterium fractionation. Likely, this reprocessing of the water occurred in the warm surface layers of protoplanetary disks—on a disk-wide scale—where radiation from the young star photo-desorbs H_2O from preexisting ices and reforms water through gas phase reactions. The variation in measured D/H ratios for various astronomical objects provides important clues to the formation conditions at different locations in nascent planetary systems. *SALTUS* will help to unravel the following questions: What is the HDO/H_2O ratio in protoplanetary disks and how does that depend on the characteristics of the protostar, the conditions in the protoplanetary disk, and the molecular core environment? What processes play a role in the water cycle of protoplanetary disks?

SALTUS will detect deuterated isotopologues of complex organics in hot corino and non-hot corino sources. While a 1-h HiRX integration will provide $>5\sigma$ detections of single deuterated CH_3OCH_3, double deuterated CH_3OCH_3, and single deuterated C_2H_5OH in hot corinos,

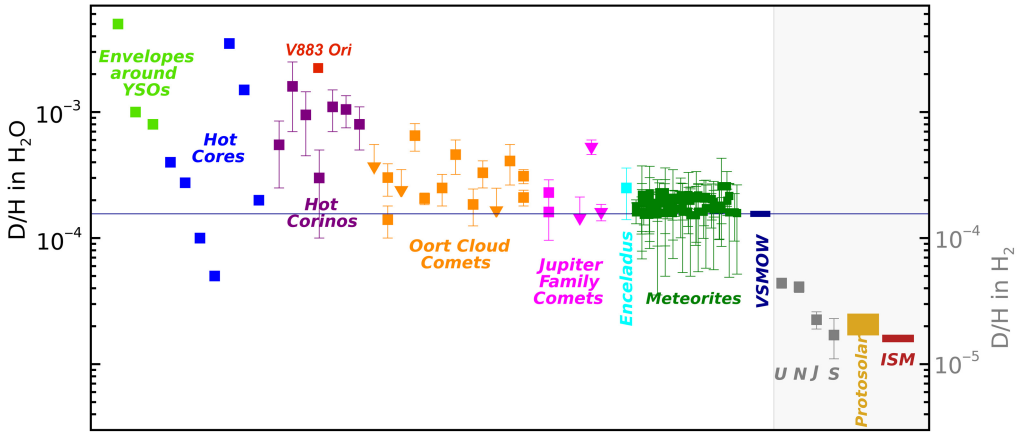

Fig. 7 Measured D/H ratios in various Galactic and solar system sources. D/H values are based on measurements of HDO and H_2O (left axis) for all objects with the exception of the solar system gas giants, the protosolar nebula, and the ISM, where the D/H values are based on HD/H_2. D/H from HD/H_2 trace the dominant reservoir of deuterium, whereas H_2O-based measurements provide insight into the chemical history of H_2O. The D/H ratio of Earth's water, as measured by VSMOW is shown by the navy rectangle. Figure patterned after,[103] in turn adapted from Refs. 104–106. Values are taken from Refs. 56 and 107–125.

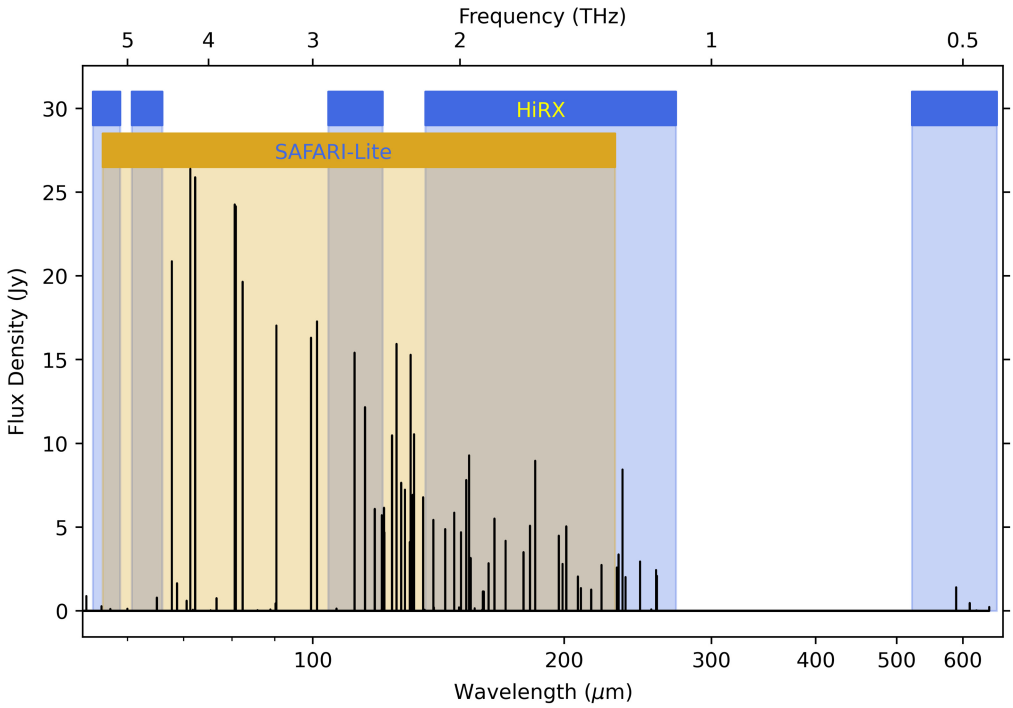

Fig. 8 Predicted HDO line emission in TW Hya, based on the best fit physical/chemical disk model of Ref. 24 and assuming $HDO/H_2O = 2 \times 10^{-3}$.

a 10-min integration will yield a robust detection of the strongest lines of deuterated molecules in protostellar envelopes.

The D/H ratio in protoplanetary disks has been probed primarily through trace species such as DCO^+ and DCN.[128–130] ALMA observations have constrained the D/H ratio in water for one disk, V883 Ori, based on detections of HDO and $H_2^{18}O$ at 200 GHz.[107] In this system, the D/H ratio was found to be similar to that for water in the ISM. However, V883 Ori is an exceptionally warm disk currently undergoing an accretion burst, thus increasing the observable water column. The main isotopologues of water are difficult to observe from ground-based facilities, even at high altitude, though $H_2^{16}O$ was recently detected in the young HL Tau disk.[131] Such observatories are often limited to the much weaker $H_2^{18}O$ lines, which are still impacted by the low atmospheric transmission at the relevant frequencies.[108] We identify the strongest transitions of HDO using the physical/chemical disk model of Ref. 24 (Fig. 8). This model of the nearby disk TW Hya reproduces the resolved ALMA observations of multiple CO transitions as well as the total HD 1-0 flux from *Herschel*, and the upper limits on the HDO 225 GHz line from the submillimeter array (SMA).[7,132] The strongest HDO transitions in protoplanetary disks are at 71.4 μm and inaccessible from the ground. These observations will provide the link between water in the ISM to water in planetary systems, providing a definitive answer to whether water on terrestrial planets is commonly inherited from the ISM.

2.6 Debris Disks

The debris disk phase follows the protoplanetary disk phase. Debris disks are gas-poor, with broad disks or rings of second-generation dust thought to be influenced by the presence of planets (e.g., Ref. 133). Debris disk observations allow us to study populations of small bodies around other stars and infer the presence of planets that otherwise evade detection.[134,135] They also provide insight into the composition of solid bodies in other planetary systems.[136,137] Debris disks may play a role in planet formation because of the gas (with total masses up to $\sim 1\,M_\oplus$) that is now observed in these disks (e.g., Ref. 138). Indeed, this gas could spread and accrete onto planets, thus changing their initial atmospheric compositions between 10 and 100 Myr.[139] This secondary gas component may also be important to understand our own Solar System and find out whether the Kuiper belt can still release gas today or whether it may

have contained gas in its youth.[140] If this gas could get accrete onto the giants, it may explain, e.g., the high metallicity of Uranus and Neptune.[139] *SALTUS* has the potential to observe Kuiper Belt analogs, which is necessary to be able to explore these questions.

2.6.1 *Kuiper belt analogues*

Debris disks with the same intrinsic luminosity as the Solar System's Kuiper Belt have yet to be observed.[141] These exo-Kuiper Belts have typical temperatures of ~50 K, corresponding to a black-body emission peak in the far-IR. Updating sensitivity estimates from the original *SPICA* SAFARI[142] to *SALTUS*'s SAFARI-Lite, *SALTUS* will reach the 5σ sensitivity threshold to detect exo-Kuiper belts around the nearest 30 G and K stars with known debris disks in 1 h of integration. *SALTUS* can determine the frequency of exo-Kuiper Belts, characterizing how common dust is in mature planetary systems, thus addressing Decadal Question E-Q1d. In addition, the angular resolution of *SALTUS* should enable mapping of the dust in some of these systems, thereby serving as a Rosetta Stone between the far-IR and longer wavelength observations of ALMA. It is possible that the massive exo-Kuiper belts detected to date prevent the development of life in the habitable zone due to an excessively high bombardment rate. In this case, targeting systems with belts similar to ours (i.e., with low masses) could help optimize the search for life on another planet.

2.6.2 *Gas in debris disks*

SALTUS can observe the gas content in debris disks, which are expected to contain detectable levels of carbon and oxygen; based on the gas production model developed by Refs. 142 and 143. These observations, focusing on ionized carbon and neutral oxygen, will complement those made by ALMA, which targets CO and neutral carbon.[144,145] By doing so, *SALTUS* can gather valuable information about the carbon ionization fraction, a crucial factor in understanding the dynamics of gas, including determining the dominant mechanism of angular momentum transport. Possibilities include magneto-rotational instability (MRI),[146] or MHD winds, or even some hydrodynamic instabilities such as vertical shear instability (VSI) or Rossby Wave Instability (RWI).[147] These different mechanisms operate at different ionization fractions and densities and depend on the magnetic field configuration as well. Only new data for a large variety of systems will allow us to pinpoint the dominant mechanism. One can also use the spatial information (extracted from high spectral resolution) to rule out some mechanisms, as for instance, MHD winds are expected to only produce viscous expansion inwards. By contrast, turbulence will also allow the gas to extend further outward than its production source.

The low surface density in debris disks allows penetration of high photon flux from the central star, converting molecules such as CO, CO_2, and H_2O into ionized atomic carbon and oxygen via photodissociation and photoionization. By targeting [CII] and [OI] in the far-IR, *SALTUS* users gain insights into the initial species released from planetesimals by examining the C/O ratio, e.g., to investigate whether CO, CO_2, or H_2O is released, which could have strong connections with TNOs in the Solar System for which we can now probe the composition with the *JWST*.[148] These observations provide a comprehensive understanding of the gas disk composition at different radii from the central star. The accretion of carbon and oxygen by young planets may play a pivotal role in the formation of the building blocks of life[149,150] or affect the temperature through greenhouse effects, thus influencing their habitability. Currently, debris disk studies have been mainly with A stars.[23] *SALTUS* has the sensitivity to detect [CII] and [OI] in the more common FGK stars. These observations determine the C/O ratio across spectral type during the late stages of planet formation, when volatile gasses are delivered to terrestrial planets, and address Decadal Question E-Q3a "How are potentially habitable environments formed?" *SALTUS* can particularly look at this question around solar mass stars.

3 Summary

The far-IR regime covers many unique tracers of star and planet formation, such as the ground state transitions of H_2O and HD, and emission features from ice phonon modes. With its

unprecedented sensitivity and resolution, *SALTUS* is designed to leverage these tracers to address many of the high-priority questions identified by Astro2020.[4] We have detailed how *SALTUS* will use HD 1-0 and 2-1, tracing gas mass, along with multiple optically thick H_2O and CO lines, tracing temperature, to measure the gas mass of hundreds of protoplanetary disks. Using the high spectral resolution HiRX instrument, *SALTUS* will map the abundance and distribution of H_2O vapor in disks, whereas the SAFARI-Lite instrument will observe H_2O ice phonon modes, yielding H_2O ice abundances. *SALTUS* also covers many transitions from carbon, hydrogen, oxygen, nitrogen, and sulfur (CHONS) bearing molecules. *SALTUS* can carry out sensitive surveys of chemical complexity across evolutionary stages from prestellar cores to disks, as well as trace the formation history of water by measuring D/H ratios. At the debris disk stage, *SALTUS* is able to measure carbon-to-oxygen ratios via observations of [CII] and [OI], as well as determine the frequency of Kuiper Belt analogs around G and K stars. In conclusion, *SALTUS* will open a new window into our understanding of star and planet formation.

Disclosures

The authors have no relevant financial interests in the paper and no other potential conflicts of interest to disclose.

Code and Data Availability

This paper reviews the science cases and potential observations for a future space mission so data sharing is not applicable at this time.

References

1. C. Walker et al., "Gal/Xgal U/LDB spectroscopic/stratospheric THz observatory: GUSTO," *Proc. SPIE* **12190**, 121900E (2022).
2. G. Coppi et al., "The BLAST observatory: a sensitivity study for far-IR balloon-borne polarimeters," *Publ. Astron. Soc. Pac.* **136**, 035003 (2024).
3. C. K. Walker et al., "Orbiting Astronomical Satellite for Investigating Stellar Systems (OASIS): following the water trail from the interstellar medium to oceans," *Proc. SPIE* **11820**, 118200O (2021).
4. C. Kouveliotou et al., "Enduring quests-daring visions (NASA astrophysics in the next three decades)," arXiv:1401.3741 (2014).
5. P. J. Armitage, *Astrophysics of Planet Formation*, 2nd ed., Cambridge University Press (2020).
6. P. F. Goldsmith, E. A. Bergin, and D. C. Lis, "Carbon monoxide and dust column densities: the dust-to-gas ratio and structure of three giant molecular cloud cores," *Astrophys. J.* **491**, 615–637 (1997).
7. E. A. Bergin et al., "An old disk still capable of forming a planetary system," *Nature* **493**, 644–646 (2013).
8. M. K. McClure et al., "Mass measurements in protoplanetary disks from hydrogen deuteride," *Astrophys. J.* **831**, 167 (2016).
9. F. Du, E. A. Bergin, and M. R. Hogerheijde, "Volatile depletion in the TW Hydrae disk atmosphere," *Astrophys. J. Lett.* **807**, L32 (2015).
10. A. Miotello, S. Bruderer, and E. F. van Dishoeck, "Protoplanetary disk masses from CO isotopologue line emission," *Astron. Astrophys.* **572**, A96 (2014).
11. K. R. Schwarz et al., "Unlocking CO depletion in protoplanetary disks. I. The warm molecular layer," *Astrophys. J.* **856**, 85 (2018).
12. K. Zhang et al., "Systematic variations of CO gas abundance with radius in gas-rich protoplanetary disks," *Astrophys. J.* **883**, 98 (2019).
13. A. Miotello et al., "Setting the stage for planet formation: measurements and implications of the fundamental disk properties," *Astron. Soc. Pac. Conf. Ser.* **534**, 501 (2023).
14. D. E. Anderson et al., "Probing the gas content of late-stage protoplanetary disks with N_2H^+," *Astrophys. J.* **881**, 127 (2019).
15. L. Trapman et al., "A novel way of measuring the gas disk mass of protoplanetary disks using N_2H^+ and $C^{18}O$," *Astrophys. J. Lett.* **926**, L2 (2022).
16. L. I. Cleeves, F. C. Adams, and E. A. Bergin, "Exclusion of cosmic rays in protoplanetary disks: stellar and magnetic effects," *Astrophys. J.* **772**, 5 (2013).
17. Y. Aikawa et al., "Molecules with ALMA at Planet-forming Scales (MAPS). XIII. HCO^+ and disk ionization structure," *Astrophys. J. Suppl. Ser.* **257**, 13 (2021).
18. D. E. Long et al., "Exploring the complex ionization environment of the turbulent DM tau disk," *Astrophys. J.* **972**, 88 (2024).

19. B. Veronesi et al., "A dynamical measurement of the disk mass in elias 227," *Astrophys. J. Lett.* **914**, L27 (2021).
20. S. M. Andrews et al., "On kinematic measurements of self-gravity in protoplanetary disks," *Astrophys. J.* **970**(2), 153 (2024).
21. E. A. Bergin and J. P. Williams, *The determination of protoplanetary disk masses*, Vol. 445, Springer (2017).
22. L. Trapman et al., "Far-infrared HD emission as a measure of protoplanetary disk mass," *Astron. Astrophys.* **605**, A69 (2017).
23. I. Kamp et al., "The formation of planetary systems with SPICA," *Publ. Astron. Soc. Aust.* **38**, e055 (2021).
24. J. K. Calahan et al., "The TW Hya Rosetta Stone Project. III. Resolving the gaseous thermal profile of the disk," *Astrophys. J.* **908**, 8 (2021).
25. K. R. Schwarz et al., "The radial distribution of H_2 and CO in TW Hya as revealed by resolved ALMA observations of CO isotopologues," *Astrophys. J.* **823**, 91 (2016).
26. K. R. Schwarz et al., "Protoplanetary disk science with the Orbiting Astronomical Satellite Investigating Stellar Systems (OASIS) observatory," *Space Sci. Rev.* **219**, 12 (2023).
27. I. Kamp et al., "Continuum and line modelling of discs around young stars. II. Line diagnostics for GASPS from the DENT grid," *Astron. Astrophys.* **532**, A85 (2011).
28. D. Fedele et al., "DIGIT survey of far-infrared lines from protoplanetary disks. I. [O i], [C ii], OH, H_2O, and CH^+," *Astron. Astrophys.* **559**, A77 (2013).
29. C. F. Manara et al., "Demographics of young stars and their protoplanetary disks: lessons learned on disk evolution and its connection to planet formation," *Astron. Soc. Pac. Conf. Ser.* **534**, 539 (2023).
30. M. R. Hogerheijde et al., "Detection of the water reservoir in a forming planetary system," *Science* **334**, 338 (2011).
31. F. Du et al., "Survey of cold water lines in protoplanetary disks: indications of systematic volatile depletion," *Astrophys. J.* **842**, 98 (2017).
32. A. Banzatti et al., "Hints for icy pebble migration feeding an oxygen-rich chemistry in the inner planet-forming region of disks," *Astrophys. J.* **903**, 124 (2020).
33. P. Mollière et al., "Interpreting the atmospheric composition of exoplanets: sensitivity to planet formation assumptions," *Astrophys. J.* **934**, 74 (2022).
34. K. I. Oberg, R. Murray-Clay, and E. Bergin, "The effects of snowlines on C/O in planetary atmospheres," *Astrophys. J. Lett.* **743**(1), L16 (2011).
35. G. Perotti et al., "Water in the terrestrial planet-forming zone of the PDS 70 disk," *Nature* **620**, 516–520 (2023).
36. D. Gasman et al., "MINDS. Abundant water and varying C/O across the disk of Sz 98 as seen by JWST/MIRI," *Astron. Astrophys.* **679**, A117 (2023).
37. J. A. Sturm et al., "A JWST inventory of protoplanetary disk ices. The edge-on protoplanetary disk HH 48 NE, seen with the Ice Age ERS program," *Astron. Astrophys.* **679**, A138 (2023).
38. A. Banzatti et al., "JWST reveals excess cool water near the snow line in compact disks, consistent with pebble drift," *Astrophys. J. Lett.* **957**, L22 (2023).
39. M. Meixner et al., "Origins space telescope mission concept study report," arXiv:1912.06213 (2019).
40. D. N. C. Lin, P. Bodenheimer, and D. C. Richardson, "Orbital migration of the planetary companion of 51 Pegasi to its present location," *Nature* **380**, 606–607 (1996).
41. S. N. Raymond and A. Izidoro, "Origin of water in the inner solar system: planetesimals scattered inward during Jupiter and Saturn's rapid gas accretion," *Icarus* **297**, 134–148 (2017).
42. C. W. Ormel et al., "Dust coagulation and fragmentation in molecular clouds. I. How collisions between dust aggregates alter the dust size distribution," *Astron. Astrophys.* **502**, 845–869 (2009).
43. S. Notsu et al., "Candidate water vapor lines to locate the H_2O snowline through high-dispersion spectroscopic observations. I. The case of a T Tauri Star," *Astrophys. J.* **827**, 113 (2016).
44. M. Temmink et al., "MINDS. The DR Tau disk II: probing the hot and cold H_2O reservoirs in the JWST-MIRI spectrum," *Astron. Astrophys.* **689**, 17 (2024).
45. S. Krijt, F. J. Ciesla, and E. A. Bergin, "Tracing water vapor and ice during dust growth," *Astrophys. J.* **833**, 285 (2016).
46. A. D. Bosman and E. A. Bergin, "Reimagining the water snowline," *Astrophys. J. Lett.* **918**, L10 (2021).
47. G. M. Kennedy and S. J. Kenyon, "Planet formation around stars of various masses: the snow line and the frequency of giant planets," *Astrophys. J.* **673**, 502–512 (2008).
48. R. B. Fernandes et al., "Hints for a turnover at the snow line in the giant planet occurrence rate," *Astrophys. J.* **874**, 81 (2019).
49. M. Min et al., "The abundance and thermal history of water ice in the disk surrounding HD 142527 from the DIGIT Herschel Key Program," *Astron. Astrophys.* **593**, A11 (2016).
50. J. A. Sturm et al., "The edge-on protoplanetary disk HH 48 NE. II. Modeling ices and silicates," *Astron. Astrophys.* **677**, A18 (2023).

51. E. A. Bergin and M. Tafalla, "Cold dark clouds: the initial conditions for star formation," *Annu. Rev. Astron. Astrophys.* **45**, 339–396 (2007).
52. P. André et al., "From filamentary networks to dense cores in molecular clouds: toward a new paradigm for star formation," in *Protostars and Planets VI*, H. Beuther et al., Eds., pp. 27–51 (2014).
53. J. E. Pineda et al., "From bubbles and filaments to cores and disks: gas gathering and growth of structure leading to the formation of stellar systems," *Astron. Soc. Pac. Conf. Ser.* **534**, 233 (2023).
54. S. S. Jensen et al., "Modeling chemistry during star formation: water deuteration in dynamic star-forming regions," *Astron. Astrophys.* **649**, A66 (2021).
55. E. A. Bergin and R. L. Snell, "Sensitive limits on the water abundance in cold low-mass molecular cores," *Astrophys. J. letters* **581**, L105–L108 (2002).
56. E. F. van Dishoeck et al., "Water in star-forming regions: physics and chemistry from clouds to disks as probed by Herschel spectroscopy," *Astron. Astrophys.* **648**, A24 (2021).
57. I. Evans et al., "Tracing the mass during low-mass star formation. II. Modeling the submillimeter emission from preprotostellar cores," *Astrophys. J.* **557**, 193–208 (2001).
58. S. S. Prasad and S. P. Tarafdar, "UV radiation field inside dense clouds - its possible existence and chemical implications," *Astrophys. J.* **267**, 603–609 (1983).
59. P. Caselli et al., "First detection of water vapor in a pre-stellar core," *Astrophys. J. Lett.* **759**, L37 (2012).
60. K. E. Young et al., "Probing pre-protostellar cores with formaldehyde," *Astrophys. J.* **614**, 252–266 (2004).
61. F. F. S. van der Tak, E. F. van Dishoeck, and P. Caselli, "Abundance profiles of CH_3OH and H_2CO toward massive young stars as tests of gas-grain chemical models," *Astron. Astrophys.* **361**, 327–339 (2000).
62. M. Morris, P. Palmer, and B. Zuckerman, "Hot ammonia in Orion," *Astrophys. J.* **237**, 1–8 (1980).
63. G. A. Blake et al., "Molecular abundances in OMC-1: the chemical composition of interstellar molecular clouds and the influence of massive star formation," *Astrophys. J.* **315**, 621 (1987).
64. R. T. Garrod and E. Herbst, "Formation of methyl formate and other organic species in the warm-up phase of hot molecular cores," *Astron. Astrophys.* **457**, 927–936 (2006).
65. E. Herbst and E. F. van Dishoeck, "Complex organic interstellar molecules," *Annu. Rev. Astron. Astrophys.* **47**, 427–480 (2009).
66. R. T. Garrod and S. L. Widicus Weaver, "Simulations of hot-core chemistry," *Chem. Rev.* **113**, 8939–8960 (2013).
67. J. B. Bergner et al., "Astrochemistry with the Orbiting Astronomical Satellite for Investigating Stellar Systems (OASIS)," *Front. Astron. Space Sci.* **8**, 246 (2022).
68. B. A. McGuire et al., "First results of an ALMA band 10 spectral line survey of NGC 6334I: detections of glycolaldehyde ($HC(O)CH_2OH$) and a new compact bipolar outflow in HDO and CS," *Astrophys. J. Lett.* **863**, L35 (2018).
69. N. R. Crockett et al., "Herschel observations of extraordinary sources: analysis of the HIFI 1.2 THz wide spectral survey toward Orion KL. I. Methods," *Astrophys. J.* **787**, 112 (2014).
70. J. L. Neill et al., "Herschel observations of extraordinary sources: analysis of the full Herschel/HIFI molecular line survey of Sagittarius B2(N)," *Astrophys. J.* **789**, 8 (2014).
71. G. Garay et al., "Molecular abundance enhancements in the highly collimated bipolar outflow BHR 71," *Astrophys. J.* **509**, 768–784 (1998).
72. C. Codella and R. Bachiller, "Molecular outflows in intermediate-mass star forming regions: the case of CB3," *Astron. Astrophys.* **350**, 659–671 (1999).
73. M. A. Requena-Torres et al., "Organic chemistry in the dark clouds L1448 and L183: a unique grain mantle composition," *Astrophys. J. Lett.* **655**, L37–L40 (2007).
74. H. G. Arce et al., "Complex molecules in the L1157 molecular outflow," *Astrophys. J. Lett.* **681**, L21 (2008).
75. C. Ceccarelli et al., "Herschel spectral surveys of star-forming regions. Overview of the 555-636 GHz range," *Astron. Astrophys.* **521**, L22 (2010).
76. C. Codella et al., "The CHESS spectral survey of star forming regions: peering into the protostellar shock L1157-B1. I. Shock chemical complexity," *Astron. Astrophys.* **518**, L112 (2010).
77. A. Tielens, *Molecular astrophysics*, Cambridge University Press (2021).
78. A. M. Burkhardt et al., "Modeling C-shock chemistry in isolated molecular outflows," *Astrophys. J.* **881**, 32 (2019).
79. T. Yamaguchi et al., "Detection of phosphorus nitride in the Lynds 1157 B1 shocked region," *PASJ* **63**, L37–L41 (2011).
80. J. B. Bergner et al., "Detection of phosphorus-bearing molecules toward a solar-type protostar," *Astrophys. J. Lett.* **884**, L36 (2019).
81. I. Jiménez-Serra et al., "The chemistry of phosphorus-bearing molecules under energetic phenomena," *Astrophys. J.* **862**, 128 (2018).
82. K. I. Öberg et al., "The Spitzer ice legacy: ice evolution from cores to protostars," *Astrophys. J.* **740**, 109 (2011).

83. A. Dutrey, S. Guilloteau, and M. Guelin, "Chemistry of protosolar-like nebulae: the molecular content of the DM Tau and GG Tau disks.," *Astron. Astrophys.* **317**, L55–L58 (1997).
84. K. I. Öberg et al., "The comet-like composition of a protoplanetary disk as revealed by complex cyanides," *Nature* **520**, 198–201 (2015).
85. V. V. Guzmán et al., "Nitrogen fractionation in protoplanetary disks from the H13CN/HC15N ratio," *Astrophys. J.* **836**, 30 (2017).
86. J. B. Bergner et al., "A survey of C_2H, HCN, and $C^{18}O$ in protoplanetary disks," *Astrophys. J.* **876**, 25 (2019).
87. S. E. van Terwisga et al., "The ALMA Lupus protoplanetary disk survey: evidence for compact gas disks and molecular rings from CN," *Astron. Astrophys.* **623**, A150 (2019).
88. V. N. Salinas et al., "First detection of gas-phase ammonia in a planet-forming disk. NH_3, N_2H^+, and H_2O in the disk around TW Hydrae," *Astron. Astrophys.* **591**, A122 (2016).
89. J. R. Najita et al., "High-resolution mid-infrared spectroscopy of GV tau N: surface accretion and detection of NH_3 in a young protoplanetary disk," *Astrophys. J.* **908**, 171 (2021).
90. K. Zhang et al., "Tracing the water snowline in protoplanetary disks with the ngVLA," *Astron. Soc. Pac. Conf. Ser.* **517**, 209 (2018).
91. A. Dutrey et al., "Chemistry in disks. V. Sulfur-bearing molecules in the protoplanetary disks surrounding LkCa15, MWC480, DM Tauri, and GO Tauri," *Astron. Astrophys.* **535**, A104 (2011).
92. S. Guilloteau et al., "A sensitive survey for ^{13}CO, CN, H_2CO, and SO in the disks of T Tauri and Herbig Ae stars," *Astron. Astrophys.* **549**, A92 (2013).
93. R. Le Gal et al., "Sulfur chemistry in protoplanetary disks: CS and H_2CS," *Astrophys. J.* **876**, 72 (2019).
94. N. T. Phuong et al., "First detection of H_2S in a protoplanetary disk. The dense GG Tauri A ring," *Astron. Astrophys.* **616**, L5 (2018).
95. P. Rivière-Marichalar et al., "H_2S observations in young stellar disks in Taurus," *Astron. Astrophys.* **652**, A46 (2021).
96. P. Rivière-Marichalar et al., "AB Aur, a Rosetta stone for studies of planet formation. II. H_2S detection and sulfur budget," *Astron. Astrophys.* **665**, A61 (2022).
97. K. R. Schwarz and E. A. Bergin, "The effects of initial abundances on nitrogen in protoplanetary disks," *Astrophys. J.* **797**, 113 (2014).
98. K. M. Pontoppidan et al., "The nitrogen carrier in inner protoplanetary disks," *Astrophys. J.* **874**, 92 (2019).
99. D. P. O'Brien et al., "Water delivery and giant impacts in the 'Grand Tack' scenario," *Icarus* **239**, 74–84 (2014).
100. M. W. Broadley et al., "Origin of life-forming volatile elements in the inner Solar System," *Nature* **611**, 245–255 (2022).
101. R. Hagemann, G. Nief, and E. Roth, "Absolute isotopic scale for deuterium analysis of natural waters. Absolute D/H ratio for SMOW," *Tellus* **22**, 712–715 (1970).
102. T. Prodanović, G. Steigman, and B. D. Fields, "The deuterium abundance in the local interstellar medium," *Mon. Not. R. Astron. Soc.* **406**, 1108–1115 (2010).
103. C. M. Anderson et al., "Solar system science with the Orbiting Astronomical Satellite Investigating Stellar Systems (OASIS) observatory," *Space Sci. Rev.* **218**, 43 (2022).
104. P. Hartogh et al., "Direct detection of the Enceladus water torus with Herschel," *Astron. Astrophys.* **532**, L2 (2011).
105. D. C. Lis et al., "A Herschel study of D/H in water in the Jupiter-family Comet 45P/Honda-Mrkos-Pajdušáková and prospects for D/H measurements with CCAT," *Astrophys. J. Lett.* **774**, L3 (2013).
106. D. Bockelée-Morvan et al., "Herschel measurements of the D/H and $^{16}O/^{18}O$ ratios in water in the Oort-cloud comet C/2009 P1 (Garradd)," *Astron. Astrophys.* **544**, L15 (2012).
107. J. J. Tobin et al., "Deuterium-enriched water ties planet-forming disks to comets and protostars," *Nature* **615**, 227–230 (2023).
108. F. F. S. van der Tak et al., "Water in the envelopes and disks around young high-mass stars," *Astron. Astrophys.* **447**, 1011–1025 (2006).
109. S. S. Jensen et al., "ALMA observations of water deuteration: a physical diagnostic of the formation of protostars," *Astron. Astrophys.* **631**, A25 (2019).
110. N. Biver et al., "Isotopic ratios of H, C, N, O, and S in comets C/2012 F6 (Lemmon) and C/2014 Q2 (Lovejoy)," *Astron. Astrophys.* **589**, A78 (2016).
111. G. L. Villanueva et al., "A sensitive search for deuterated water in Comet 8p/Tuttle," *Astrophys. J. Lett.* **690**, L5–L9 (2009).
112. L. Paganini et al., "Ground-based detection of deuterated water in comet C/2014 Q2 (Lovejoy) at IR wavelengths," *Astrophys. J. Lett.* **836**, L25 (2017).
113. D. C. Lis et al., "Terrestrial deuterium-to-hydrogen ratio in water in hyperactive comets," *Astron. Astrophys.* **625**, L5 (2019).

114. A. Coutens et al., "A study of deuterated water in the low-mass protostar IRAS 16293-2422," *Astron. Astrophys.* **539**, A132 (2012).
115. A. Coutens et al., "Deuterated water in the solar-type protostars NGC 1333 IRAS 4A and IRAS 4B," *Astron. Astrophys.* **560**, A39 (2013).
116. A. Coutens et al., "Water deuterium fractionation in the high-mass star-forming region G34.26+0.15 based on Herschel/HIFI data," *Mon. Not. R. Astron. Soc.* **445**, 1299–1313 (2014).
117. M. V. Persson et al., "The deuterium fractionation of water on solar-system scales in deeply-embedded low-mass protostars," *Astron. Astrophys.* **563**, A74 (2014).
118. K. S. Wang, F. F. S. van der Tak, and M. R. Hogerheijde, "Kinematics of the inner thousand AU region around the young massive star AFGL 2591-VLA3: a massive disk candidate?," *Astron. Astrophys.* **543**, A22 (2012).
119. M. Emprechtinger et al., "The abundance, ortho/para ratio, and deuteration of water in the high-mass star-forming region NGC 6334 I," *Astrophys. J.* **765**, 61 (2013).
120. F. P. Helmich, E. F. van Dishoeck, and D. J. Jansen, "The excitation and abundance of HDO toward W3(OH)/(H_2O)," *Astron. Astrophys.* **313**, 657–663 (1996).
121. L. Bonal et al., "Hydrogen isotopic composition of the water in CR chondrites," *Geochim. Cosmochem. Acta* **106**, 111–133 (2013).
122. L. Yang, F. J. Ciesla, and C. M. O. D. Alexander, "The D/H ratio of water in the solar nebula during its formation and evolution," *Icarus* **226**, 256–267 (2013).
123. E. Jacquet and F. Robert, "Water transport in protoplanetary disks and the hydrogen isotopic composition of chondrites," *Icarus* **223**, 722–732 (2013).
124. E. L. Gibb et al., "An infrared search for HDO in Comet D/2012 S1 (ISON) and implications for iSHELL," *Astrophys. J.* **816**, 101 (2016).
125. N. Biver, R. Moreno, and D. Bockelée-Morvan, "HDO in comet 46p/Wirtanen from ALMA observations," in prep (2024).
126. A. G. G. M. Tielens, "Surface chemistry of deuterated molecules," *Astron. Astrophys.* **119**, 177–184 (1983).
127. C. Ceccarelli et al., "Deuterium fractionation: the ariadne's thread from the precollapse phase to meteorites and comets today," in *Protostars and Planets VI*, H. Beuther et al., Eds., pp. 859–882, The University of Arizona Press (2014).
128. J. Huang et al., "An ALMA survey of DCN/$H^{13}CN$ and $DCO^+/H^{13}CO^+$ in protoplanetary disks," *Astrophys. J.* **835**, 231 (2017).
129. V. N. Salinas et al., "DCO^+, DCN, and N^2D^+ reveal three different deuteration regimes in the disk around the Herbig Ae star HD 163296," *Astron. Astrophys.* **606**, A125 (2017).
130. C. E. Muñoz-Romero et al., "Cold deuterium fractionation in the nearest planet-forming disk," *Astrophys. J.* **943**, 35 (2023).
131. S. Facchini et al., "Resolved ALMA observations of water in the inner astronomical units of the HL Tau disk," *Nat. Astron.* (2024).
132. C. Qi et al., "Resolving the chemistry in the disk of TW hydrae. I. Deuterated species," *Astrophys. J.* **681**, 1396–1407 (2008).
133. T. D. Pearce et al., "Planet populations inferred from debris discs. Insights from 178 debris systems in the ISPY, LEECH, and LIStEN planet-hunting surveys," *Astron. Astrophys.* **659**, A135 (2022).
134. A. M. Lagrange et al., "A giant planet imaged in the disk of the young star β Pictoris," *Science* **329**, 57 (2010).
135. N. Skaf et al., "The β Pictoris system: setting constraints on the planet and the disk structures at mid-IR wavelengths with NEAR," *Astron. Astrophys.* **675**, A35 (2023).
136. T. Mittal et al., "The spitzer infrared spectrograph debris disk catalog. II. Silicate feature analysis of unresolved targets," *Astrophys. J.* **798**, 87 (2015).
137. T. J. Rodigas et al., "On the morphology and chemical composition of the HR 4796A debris disk," *Astrophys. J.* **798**, 96 (2015).
138. A. Moór et al., "Molecular gas in debris disks around young A-TYPE Stars," *Astrophys. J.* **849**, 123 (2017).
139. Q. Kral, J. Davoult, and B. Charnay, "Formation of secondary atmospheres on terrestrial planets by late disk accretion," *Nat. Astron* **4**, 769–775 (2020).
140. Q. Kral et al., "A molecular wind blows out of the Kuiper belt," *Astron. Astrophys.* **653**, L11 (2021).
141. C. Eiroa et al., "DUst around NEarby stars. The survey observational results," *Astron. Astrophys.* **555**, A11 (2013).
142. Q. Kral et al., "Predictions for the secondary CO, C and O gas content of debris discs from the destruction of volatile-rich planetesimals," *Mon. Not. R. Astron. Soc.* **469**, 521–550 (2017).
143. Q. Kral et al., "Imaging [CI] around HD 131835: reinterpreting young debris discs with protoplanetary disc levels of CO gas as shielded secondary discs," *Mon. Not. R. Astron. Soc.* **489**, 3670–3691 (2019).

144. Q. Kral et al., "A self-consistent model for the evolution of the gas produced in the debris disc of β Pictoris," *Mon. Not. R. Astron. Soc.* **461**, 845–858 (2016).
145. G. Cataldi et al., "The surprisingly low carbon mass in the debris disk around HD 32297," *Astrophys. J.* **892**, 99 (2020).
146. Q. Kral and H. Latter, "The magnetorotational instability in debris-disc gas," *Mon. Not. R. Astron. Soc.* **461**, 1614–1620 (2016).
147. C. Cui et al., "Dynamics of cold circumstellar gas in debris discs," *Mon. Not. R. Astron. Soc.* **530**, 1766–1780 (2024).
148. M. N. De Prá et al., "Widespread CO_2 and CO ices in the trans-Neptunian population revealed by JWST/DiSCo-TNOs," *Nat. Astron.* (2024).
149. R. S. Sutherland and M. A. Dopita, "Effects of preionization in radiative shocks. I. Self-consistent models," *Astrophys. J. Suppl.* **229**, 34 (2017).
150. C. H. M. Pabst et al., "[C II] 158 μm line emission from Orion A I. A template for extragalactic studies?," *Astron. Astrophys.* **651**, A111 (2021).

Kamber R. Schwarz holds a postdoctoral position at the Max Planck Institute for Astronomy in Heidelberg. She was a NASA Sagan Postdoctoral Fellow at the Lunar and Planetary Laboratory at the University of Arizona. She received a PhD in Astronomy & Astrophysics at the University of Michigan in 2018. She studies the evolution of volatile gas during planet formation, with the goal of determining the amount of volatile carbon, nitrogen, and oxygen available to form planets. Her research combines observations from the infrared to the millimeter, using facilities such as ALMA, NOEMA, and JWST, with physical/chemical modeling to constrain the timescales and mechanisms of volatile reprocessing. She has authored about 100 publications.

Alexander Tielens is a professor of astronomy in the Astronomy Department of the University of Maryland, College Park. He received his MS and PhD degrees in astronomy from Leiden University in 1982. He has authored over 500 papers in refereed journals and has written two textbooks on the interstellar medium. His scientific interests center on the physics and chemistry of the interstellar medium, particularly in regions of star and planet formation.

Joan Najita is an astronomer at NSF's NOIRLab and its Head of Scientific Staff for User Support. She was formerly the Chief Scientist at the National Optical Astronomy Observatory (NOAO) and served on its scientific staff since 1998. In 1993, she received her PhD from the University of California, Berkeley. Najita has been responsible for strategic planning, science career development, science communications, and the health of the scientific environment at the Observatory. Her interests include traditional research topics (such as star and planet formation, exoplanets, and the Milky Way), advocacy for the development of new research capabilities (such as infrared spectroscopy and massively multiplexed wide-field spectroscopy), as well as the sociological context of astronomy (such as the nature of discovery in astronomy and its science sociology and resource allocation practices). She has a lifelong interest in communicating science to the public and in the role of science in society. Joan Najita has been named a 2021–2022 fellow at Harvard Radcliffe Institute, joining artists, scientists, scholars, and practitioners in a year of discovery and interdisciplinary exchange in Cambridge. She has authored about 190 publications.

Jennifer Bergner is an assistant professor of Chemistry at UC Berkeley. She received her BS degree from the University of Virginia and her MA and PhD degrees from Harvard in 2019. Her astrochemistry group uses a variety of tools to explore the chemistry at play in protostars and protoplanetary disks, the progenitors of planetary systems. With cryogenic vacuum experiments, she mimics the extremely low temperatures and pressures of star-forming regions in the lab to explore the chemical and microphysical behavior of volatile ice. She also uses state-of-the-art telescope facilities such as ALMA and JWST to observe the spectral fingerprints of volatile molecules in protostars and protoplanetary disks, providing insight into the chemical landscape of planet formation and the underlying physical processes that drive astrochemical evolution. She has about 128 publications.

Quentin Kral is an astronomer at the Paris Observatory (LESIA). His main research interests are debris disks, the solar system, and planetary formation. He is an expert on the new gas component that is now observed in mature extrasolar systems once the young planet-forming disk has

dissipated. He mainly uses ALMA to test his models and investigate the gas and dust in exoplanetary systems. He is the PI of the exoplanet.eu catalog of exoplanets. He has published over 130 articles. He received his master's degree from Ecole Normale Supérieure (ENS Paris) and his PhD from Paris Observatory in 2014.

Carrie Anderson is a research scientist at NASA Goddard Space Flight Center (GSFC). She received a BS in physics from Arizona State University in 2000 and her MS and PhD degrees in astronomy from New Mexico State University in 2003 and 2006, respectively. She is the author of more than 45 papers in refereed journals and has written one book chapter. Her research focuses on the remote sensing of planetary atmospheres, primarily in the areas of thermal structure and composition, using space- and ground-based data, in the visible, near-IR, mid-IR, far-IR, and submillimeter spectral regions. Her research also includes laboratory transmission spectroscopy measurements of ice films in a high-vacuum cryo chamber located in her Spectroscopy for Planetary ICes Environments (SPICE) laboratory at NASA GSFC.

Gordon Chin is a research scientist at NASA Goddard Space Flight Center (GSFC). He received his BA in physics from Columbia College in 1970 and his MA, MPhil, and PhD degrees in physics from Columbia University in 1972, 1974, and 1977, respectively. He is the author of more than 50 refereed journal papers. His current research interests include the development of sub-millimeter planetary flight spectrometers targeting planetary atmospheres, the lunar exosphere, and ocean world plume environments in the solar system.

David Leisawitz is an astrophysicist and Chief of the Science Proposal Support Office at NASA's Goddard Space Flight Center. He received a PhD in astronomy from the University of Texas at Austin in 1985. His primary research interests are star and planetary system formation, infrared astrophysics, wide-field spatio-spectral interferometry, and far-infrared space interferometry. He is a NASA Center Study Scientist for the Far-IR Surveyor, a Mission Scientist for the Wide-field Infrared Survey Explorer (WISE), and earlier served as deputy project scientist for the Cosmic Background Explorer (COBE) under Project Scientist and mentor Dr. John Mather. He is the principal investigator for "Wide-field Imaging Interferometry," a co-investigator on the "Balloon Experimental Twin Telescope for Infrared Interferometry (BETTII)," and a member of a three-person External Advisory Panel for the "Far Infrared Space Interferometer Critical Assessment (FISICA)," a European Commission FP7 research program. In 2004–2005, he served as a principal investigator and science team lead for the Space Infrared Interferometric Telescope (SPIRIT) mission concept study. He has authored about 300 publications.

David Wilner is a senior astrophysicist at the Smithsonian Astrophysical Observatory in the Radio and Geoastronomy Division at the Center for Astrophysics, Harvard & Smithsonian. His main research interests are circumstellar disks, the formation of planets, and the development of aperture synthesis techniques. Much of his science program makes use of radio, millimeter, and submillimeter interferometers, including the Submillimeter Array, ALMA, and the VLA. He received an AB in physics from Princeton University and a PhD in Astronomy from the University of California. He frequently lectures on imaging and deconvolution in radio astronomy. He has authored about 450 publications.

Peter Roelfsema is a senior scientist/project manager at SRON Netherlands Institute for Space Research. He has been involved in several satellite projects, currently as PM for the Dutch Athena/X-IFU contribution, and before that as PI for SPICA's SAFARI Far-IR spectrometer and as lead of the international SPICA collaboration. He was PI and ad-interim PI for Herschel/HIFI, and in the early Herschel development phase, he was one of the lead system engineers developing the Herschel ground segment concept and operational systems. Before Herschel, he led the ISO/SWS operations team in Villafranca/Spain and the SWS analysis software development team. He started his scientific career as a radio astronomer, utilizing the WSRT, VLA, and ATNF to study radio recombination lines of galactic HII regions and nearby active galaxies. With ISO and Herschel he did (Far)IR spectroscopic work on galactic HII regions, studying, e.g., PAH properties and metal abundance variations in our galaxy. He has published over 150 papers in astronomical journals and conference proceedings and supervised a number of PhD students.

Floris van der Tak is a senior scientist in the astrophysics program of the Netherlands Institute for Space Research (SRON), where his research interests include astrochemistry, the habitability of exoplanets, the physics of the interstellar medium, star formation, molecular spectroscopy, and radiative transfer. He received a PhD from Leiden University in 2000. He was the project scientist for the SPICA/SAFARI instrument. He has authored about 216 publications.

Erick Young is the principal scientist of astronomy at the Universities Space Research Association. He is a widely recognized authority on infrared astronomy and the former Science Mission Operations Director for SOFIA. He specializes in designing science instruments and has participated in many NASA space infrared astronomy missions. He was responsible for developing the far-infrared detector arrays on the Spitzer Space Telescope's Multiband Imaging Photometer for Spitzer. As SOFIA Science Mission Operations Director, he manages the airborne observatory's equipment, instruments, support facilities, and infrastructure. He was also responsible for the overall scientific productivity of the facility, including the guest investigator program. He has about 385 publications.

Christopher Walker is a professor of astronomy, optical sciences, electrical and computer engineering, aerospace and mechanical engineering, and applied mathematics at the University of Arizona (UofA). He received his MSEE from Clemson University (1980), MSEE from Ohio State University (1981), and PhD in Astronomy from the University of Arizona (1988). He has worked at TRW Aerospace and the Jet Propulsion Laboratory, was a Millikan Fellow in Physics at Caltech, and has been a faculty member at the UofA since 1991, where he has worked to advance the field of terahertz astronomy. He has supervised sixteen PhD students, led numerous NASA and NSF projects, authored/coauthored 130+ papers, and published two textbooks: "Terahertz Astronomy" and "Investigating Life in the Universe."